World Academy of Science, Engineering and Technology
International Journal of Mechanical and Mechatronics Engineering
Vol:9, No:12, 2015

The Effect of Material Properties and Volumetric Changes in Phase Transformation to the Final Residual Stress of Welding Process

Djarot B. Darmadi

***Abstract*—**The wider growing Finite Element Method (FEM) application is caused by its benefits of cost saving and environment friendly. Also, by using FEM a deep understanding of certain phenomenon can be achieved. This paper observed the role of material properties and volumetric change when Solid State Phase Transformation (SSPT) takes place in residual stress formation due to a welding process of ferritic steels through coupled Thermo-Metallurgy-Mechanical (TMM) analysis.

The correctness of FEM residual stress prediction was validated by experiment. From parametric study of the FEM model, it can be concluded that the material properties change tend to over-predicts residual stress in the weld center whilst volumetric change tend to underestimates it. The best final result is the compromise of both by incorporates them in the model which has a better result compared to a model without SSPT.

***Keywords*—**Residual stress, ferritic steels, SSPT, coupled-TMM.

I. Introduction

IT has been proved that residual stress caused some pipeline blowout which detrimental to environment [1], [2]. Considering the significant role of the residual stress, British R6 or API 570 made it compulsory to evaluate residual stress in the integrity assessment of welded structures [3]. R6 assessment procedure standard, endorsed residual stress analysis of a weld configuration through a combination of numerical modeling and residual stress measurements [4], [5]. Although residual stress measurement gives accurate results but in many occasions it is impractical to measure the residual stress in a welded structure due to the difficulties of reaching the desired position or the dimension problems of real welded structure (too large). In such cases the verified numerical method may the only reliable available method [6]. Moreover using the numerical method deep understanding of welding process, especially how it produces residual stress can be obtained. Other benefit, which is clearly seen, is cost saving when determining Welding Procedure Specification (WPS) that does not need experiment or at least limits the number of specimens. One of recent prominent numerical method for welding simulation is FEM.

In the past decades, many experiments and FEM of residual stress in a welded structure have been conducted but there are still limited literatures discussed multi-pass weld joint incorporating phase transformation effects. Meanwhile the trend shows the increasing usage of high strength ferritic steels that involves phase transformation which should be included in the numerical analysis. These high strength ferritic steels offer obvious economic benefits originating from their advantageous strength to price and weight ratios [7].

In this article, three-dimensional coupled Thermo-Metallurgy-Mechanical model is employed to predict residual stress of multi-pass weld joint in a high-strength ferritic steel. Aspects in metallurgical analysis, i.e. properties and volumetric change due to SSPT were evaluated. Experiments were carried out to validate the residual stress predictions to ensure and evaluate the accuracy of developed model.

Djarot B. Darmadi is with the Mechanical Engineering Department, University of Brawijaya, Malang, 65145 Indonesia (e-mail: b_darmadi_djarot@ub.ac.id).

II. Welding Procedures

Two 30 mm plates of high strength carbon steel (POSTEN80) with double V groves as shown in Fig. 1 was prepared. The plates have longitudinal length of 500 mm and transverse width of 250 mm. When those plates are welded together will have 500 mm width (Fig. 1).

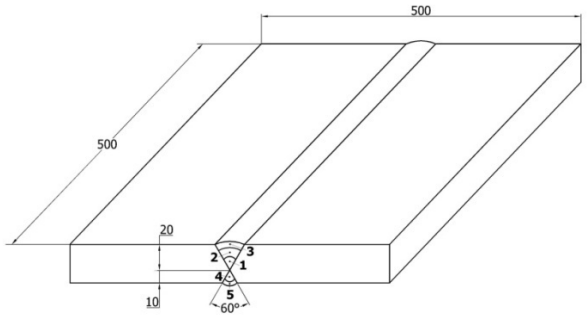

Fig. 1 Geometry and pass sequences of the welding process

TABLE I
Welding Parameters

PASS	Current [A]	Voltage [V]	Velocity [mm/s]
1	250	30	2.7
2	260	32	2.0
3	260	35	1.9
4	250	30	4.1
5	250	30	3.3

Five passes of Flux Cored Welding (FCA) were applied using 1.2 mm in diameter of filler wire (MGS80). The welding parameters for each pass are shown in Table I. Preheat temperature of 110°C was applied before first pass was carried

out. Inter-pass temperatures were 200-250°C. After the third pass the specimen was turned-over then passes 4 and 5 were applied. Chemical composition for base and filler metals is shown in Table II.

TABLE II
CHEMICAL COMPOSITION

	C	Si	Mn	P	S	Cr	Ni
BM	0,07	0,30	0,91	0,015	0,004	0,45	0,97
WM	0,05	0,44	1,35	0,006	0,001	0,60	2,3
	Cu	V	Mo	B			
BM	0,02	0,038	0,45	0,0016			
WM			0,25				

III. FINITE ELEMENT MODEL

A. Thermal Model

The shape of weld bead for each pass was approached using the melting rate equation [8] for FCAW (1).

$$MR = k + \alpha I + \frac{\beta l I^2}{A} \quad (1)$$

The melting rate – *MR* (gr/min) is the mass of filler materials melted into the welding joint. *k,* α, and β are the constants; *l* is the stick-out length and A is the cross section area of the filler materials. The relative area of the cross section of the weld-bead for each pass can be evaluated by dividing *MR* by the welding speed. A preheating temperature of 110°C for the first pass was applied and the inter-pass temperature was considered to be 200°C.

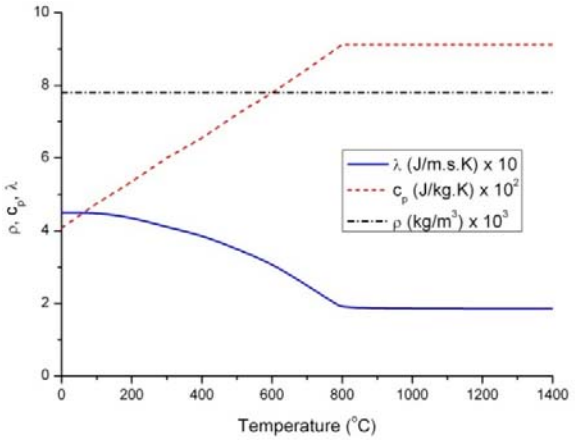

Fig. 2 Temperature dependent thermal properties of materials

TABLE III
LATENT HEAT OF SSPT AND SOLID-LIQUID TRANSFORMATION

	Latent Heat (kJ/kg)		Temperature range (°C)	
	Base	Weld	Base	Weld
Martensite	75.07	66.51	456 - 200	427 – 200
Austenite	25.35	26.27	760 – 920	
Melting	270		1450 – 1500	

Thermal properties for base metal (BM) and weld metal (WM) are temperature dependent except for density which was considered constant. Fig. 2 shows those thermal properties graphically. When SSPT takes places latent heat should be considered. The latent heat for phase and solid-liquid transformations is shown in Table III.

Volumetric heat exerted by welding torch to certain element with relative coordinate to the heat source centre (x,y,z) was modeled basically using Goldak's ellipsoidal heat source model as shown in (2) [9]:

$$\dot{q}'''_{(x,y,z)} = \frac{6\sqrt{3}EI}{\pi\sqrt{\pi}r_x.r_y.r_z} e^{-\left(\frac{3x^2}{r_x^2}+\frac{3y^2}{r_y^2}+\frac{3z^2}{r_z^2}\right)} \quad (2)$$

E and I denote voltage and current as tabulated in Table I whilst r_x, r_y and r_z are heat source parameters which equal to 5, 2, 3 mm respectively [9]–[11].

B. Metallurgy Analysis

Since thermal model significantly affects developed phase vice versa the thermal model must be coupled with the metallurgy analysis. All thermal properties were considered constant due to SSPT except the existence of latent heat as tabulated in Table III. First was modeled thermal model without SSPT. Based on temperature histories of elements in thermal model, the existed phases can be predicted. Next was run thermal model coupled with metallurgy analysis and since the latent heat was included, the temperature histories and in turn the existed phase will be altered. The existed phase and peak temperature of elements from the last run then to be compared with the previous run. This iterated step was repeated until the results were converged that is the phase configuration and peak temperature of elements from certain pass are considered equal to the previous pass.

An element which experiences austenite transformation (peak temperature exceeds A1: 760°C) when cooled down to room temperature exhibits martensite SSPT. The martensite fraction depends on real time temperature (T) follows Koistenen-Marburger law as expressed by (3) [12]. M_s is martensite start temperature which is shown in Table III.

$$f_m = 1 - e^{0.011(T-M_s)} \quad (3)$$

Although generally SSPT does not alter thermal properties but mechanical properties are change. The most important material property which affects residual stress prediction is yield stress [9]-[11], [13]. In Fig. 3 is shown temperature dependent of mechanical properties for initial materials. The linear expansion coefficient and Poisson's ratio are temperature independent equal to $1.2x10^{-5}$ (K^{-1}) and 0.3 respectively. Depend on initial phase, peak temperature, real time temperature and existed phase in Fig. 4 is shown yield stress for varied phases. Which curved is used depends on initial phase, temperature gradient (heated or cooled) and peak temperature of an observed element. If peak temperature of an element below A1, it still on the same curve. An element with initial phase of Ferrite/Pearlite and has peak temperature above A1, when cooled down to room temperature follows prime martensite curves (cooled or heated) whilst for an element with initial phase of prime martensite follows aged

martensit curves. An element with initial phase of aged martensite will always on aged martensite curves (cooled or heated).

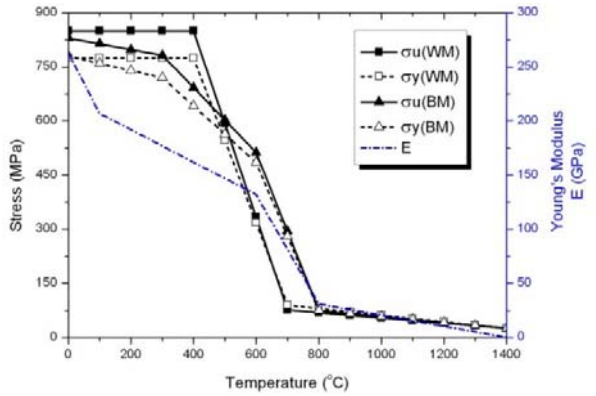

Fig. 3 Temperature dependent mechanical properties of materials

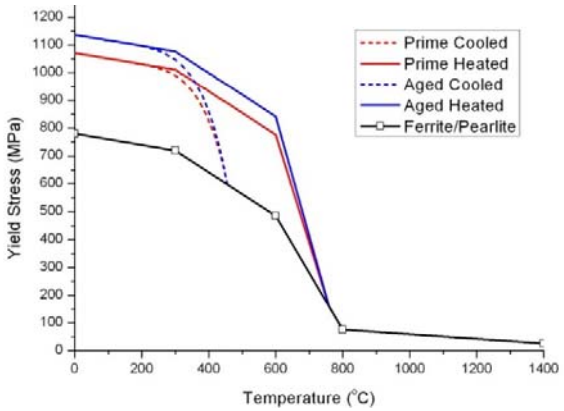

Fig. 4 (a) Yield stress of varied phase for base metal

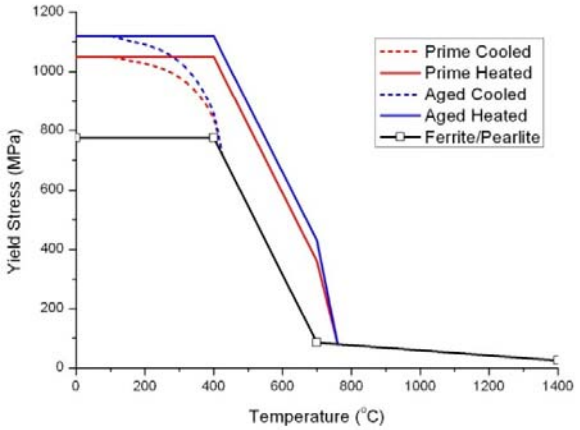

Fig. 4 (b) Yield stress of varied phase for filler metal

Beside properties' change, when SSPT is ongoing transformation plasticity should be considered. The transformation plasticity was modeled follows Desalo's normalized function as shown in (4) [14]. K is a materials constant which considered equal to 7.25e-5 [MPa^{-1}], σ is stress component in the observed direction and f_m is martensite fraction which is determined by (3).

$$\varepsilon^{tp} = K\sigma f_m(2 - f_m) \quad (4)$$

C. Mechanical Model

It is obvious that thermal results and metallurgy analysis do affect the developed stresses but does not reversely. Based on this fact, mechanical model was carried out sequentially after results from converged coupled thermo-metallurgical model have been obtained. Temperature results from thermal model were applied as temperature load in the FEM mechanical model and the material model depend on the existed phase and predicted phase which have been obtained from coupled thermo-metallurgy analysis.

Basically three unique aspects should be included in the residual stress prediction involving SSPT: properties change, transformation plasticity and volumetric change. In the metallurgy analysis section has been discussed how properties change and transformation plasticity were included in the FEM model. Volumetric change exists as a result of atomic arrangement. The atomic arrangement depends on existed phase as shown in Fig. 5. Ferrite/Pearlite has body centered cubic structure (BCC) with atomic packaging factor (APF) equal to 0.68. APF describes atomic volume per total occupied volume. Austenite has faced centered cubic structure (FCC) with APF equal 0.74. It should be noted that 0.74 is the highest possible APF that is why it is found an anomaly when ferrite/pearlite transforms to austenite that is the volume shrinks although the temperature rise. This anomaly finish when austenite transformation is ended at A3 temperature. Another anomaly is also found when martensite transformation existed that is the volume enlarges although the temperature decreases. Martensite has body centered tetragonal (BCT) structure with APF equal to 0.67 which is even lower than BCC.

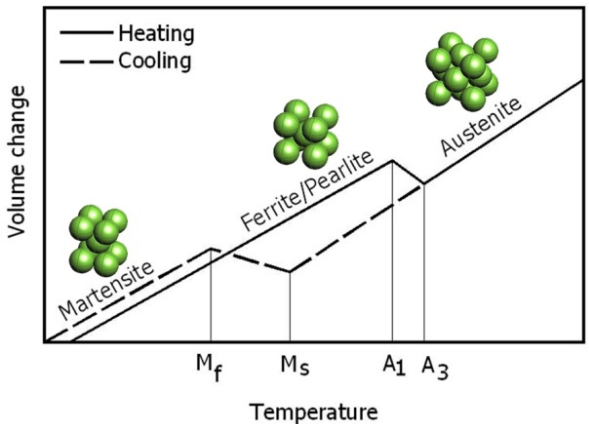

Fig. 5 Volumetric change due to SSPT

For a small temperature increment, martensite fraction difference can be obtained by integrating (3); $df_m = -0.011e^{0.011(T-M_s)}dT$. The volumetric change due to martensite phase transformation can be expressed as $\Delta\varepsilon^{sspt} = df_m$ x $\Delta\varepsilon^{mar}$ where $\Delta\varepsilon^{sspt}$ expresses the volumetric change increment and $\Delta\varepsilon^{mar}$ equal to 1.5 x 10^{-3} [15], [16] is the volumetric change of full martensite due to a solid state phase transformation.

The total volumetric change increment is a summation of volumetric change due to the martensite phase transformation and to the difference in temperature as follows.

$$\Delta\varepsilon^{T} + \Delta\varepsilon^{SSPT} = \alpha dT + \Delta\varepsilon^{mar} df_m$$
$$= 1.2x10^{-5} dT + 1.5x10^{-3}(-0.011e^{0.011(T-Ms)} dT$$
$$= \{(1.2\text{-}1.6e^{0.011(T-Ms)})10^{-5}\} dT \quad (5)$$

Using (5), Fig. 6 shows the effect of the martensite solid state phase transformation on the coefficient of thermal expansion for the base metal and weld metal. The coefficient of thermal expansion, without considering SSPT, is also plotted on the figure for a comparison. SSPT is also found when ferrite/pearlite transforms to austenite. The transformation started at A1 (760°C) and finished at A3 (920°C). The total austenitic transformation strain is 2.288 x 10^{-3} [15], [17]. For simplification, the volumetric change is considered linear, and the volumetric change for any temperature at an austenitic phase transformation range is approached using linear interpolation, as shown in (6).

$$\Delta\varepsilon^{SSPT} = \frac{\Delta T}{A_3 - A_1} \Delta\varepsilon^{aus} = \frac{-2.288\ x\ 10^{-3}}{920\,℃ - 760\,℃} \Delta T \quad (6)$$

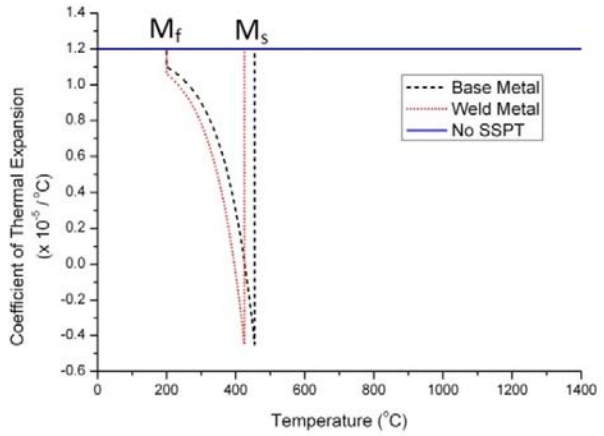

Fig. 6 Effect of martensite on the coefficient of thermal expansion

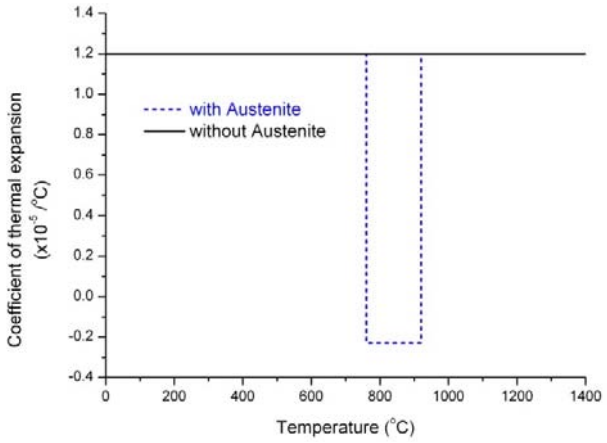

Fig. 7 Effect of austenite on the coefficient of thermal expansion

The total volumetric change is the sum of solid state phase transformation and elongation due to the temperature load, as:

$$\Delta\varepsilon^{T} + \Delta\varepsilon^{SSPT} = \alpha\Delta T + \frac{-2.288x10^{-3}}{920\,℃ - 760\,℃}\Delta T$$
$$= 1.2x10^{-5}\Delta T - 1.43x10^{-5}\Delta T$$
$$= -0.23x10^{-5}\Delta T \quad (7)$$

The effect of austenitic solid state phase transformation to the coefficient of thermal expansion is shown in Fig. 7.

IV. Results and Discussions

Using all above approaches FEM model was built. Validation was done on longitudinal residual stress which is the highest. First is evaluated the role of SSPT in the residual stress formation that is by comparing measurement results (experiment) and FEM prediction which is obtained from a model with and without SSPT phenomenon.

Fig. 8 shows a comparison between FEM predictions with and without SSPT and the experimental results to obtain a general insight into the effects of SSPT on residual stress. It can be argued from Fig. 8 that the martensitic SSPT decreased the tensile residual stress in the area close to the weld beads may due to an expansion of martensitic SSPT that occurred while the elements were cooled to room temperature. Since the expansion was constrained by the surrounding area away from the weld line, it caused compressive stress which reduced the predicted residual stress without SSPT. Fig. 8 shows that the SSPT led to a prediction that was closer to the experimental results, thus indicating that SSPT should be used to predict residual stress of high strength steels.

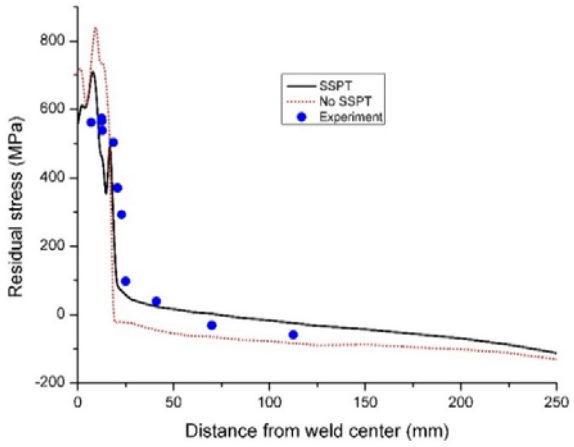

Fig. 8 Longitudinal residual stress distributed on the top path of the mid cross section area

Not only the volume but also the materials properties changed due to SSPT. Since the yield stress of martensite is higher than ferrite/pearlite, for the equal strain the residual stress should be higher which is contradictive with the effect of volumetric change. To evaluate the role of volumetric and material properties change due to SSPT, models that neglect volumetric change and material properties change respectively were simulated and the result is shown in Fig. 9.

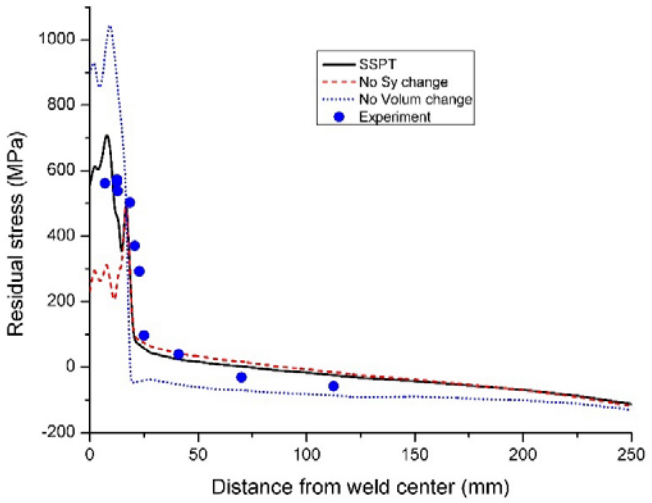

Fig. 9 Effect of yield stress and volumetric changes due to SSPT to the final residual stress

In Fig. 9 can be seen that the prediction of residual stress with SSPT is a combined result of a model with a change in material properties only (in this case is yield stress) and a model that only accommodates volumetric change. As it is expected, neglecting volumetric change due to SSPT will overestimate the residual stress close to the weld line whilst neglecting the change in material properties will give a lower prediction. Accommodating both phenomena gives intermediate results between those two cases.

V. Conclusions

The developed FEM model provided good residual stress prediction which is confirmed by results that close to experiment measurement. Predicting residual stress in high strength ferritic steels should incorporate three important unique aspect: transformation plasticity, volumetric change and material properties alteration due to SSPT. Neglecting volumetric change overestimated the final residual stress whilst neglecting material properties change underestimated it, or it can be said: volumetric change reduces residual stress while materials properties increase the residual stress close to the weld line.

References

[1] C. Manfredi and J.L. Otegui, Failures by SCC in buried pipelines, Engineering Failure Analysis, vol. 9, 2002, pp. 495 – 509.

[2] J. Wang and A. Atrens, Microstructure and grain boundary microanalysis of X70 pipeline steel, Journal of Material Science, vol.38, 2003, pp.323-330.

[3] Viorel Deaconu, Finite element modelling of residual stress – A powerfull tool in the aid of structural integrity assessment of welded structures, 5th Int. Conference Structural Integrity of Welded Structures, Romania, 2007.

[4] R6 revision 4, Assessment of the integrity of structures containing defects, British Energy Generation Ltd., 2004.

[5] AF Mark, JA Francis, H Dai, M Turski, PR Hurrell, SK Bate, JR Kornmeier and PJ Withers, On the evolution of local material properties and residual stress in a three-pass SA508 steel weld, Acta Materialia, vol. 60, 2013, pp.3268 – 3278.

[6] O. Muransky, M.C. Smith, P.J. Bendeich, T.M. Holden, V. Luzin, R.V. Martins and L. Edwards, Comprehensive numerical analysis of a three-pass bead-in-slot weld and its critical validation using neutron and synchrotron diffraction residual stress measurements, International Journal of Solids and Structures, vol.49, 2012, pp.1045 – 1062.

[7] Lenka Kuzmikova, Huijun Li, John Norrish, Zengxi Stephen Pan and Nathan Larkin, Development of safe optimized welding procedures for high strength Q&T welded with austenitic consumables, Revista Soldagem e Inspecao, vol.18, 2013, pp.169-175.

[8] John Norrish, Advanced welding processes, Woodhead Publishing in Materials, Cambridge, England, 2006.

[9] Djarot B. Darmadi, Validating the accuracy of heat source model via temperature histories and temperature field in bead-on-plate welding, International Journal of Engineering and Technology, vol.11, 2011, pp. 12-10.

[10] Djarot B. Darmadi, Anh Kiet Tieu and John Norrish, A validated thermal model of bead-on-plate welding, Heat and Mass Transfer, vol. 48, 2012, pp.1219 – 1230.

[11] Djarot B. Darmadi, Anh Kiet Tieu and John Norrish, A validated thermo mechanical FEM model of bead-on-plate welding, International Journal of Materials and Product Technology, vol.48, 2014, pp.146 – 166.

[12] D.P. Koistinen and R.E.Marburger, A general equation prescribing the extent of the austenite-martensite transformation in pure iron-carbon alloys and plain carbon steels, Acta metallurgica, vol.7, 1959, pp. 59 – 60.

[13] Djarot B. Darmadi, Study of residual stress mechanism using three elasto-plastic bars model, Asian Transactions on Engineering, Volume 01 Issue 5 (2011) 76 – 80.

[14] Y. Desalos, *Comportement Dilatometrique et Mecanique de l'Austenite Metastable d'un Acier A 533,* IRSID Report #95349401 in J.B. Leblond, J. Devaux and J.C. Devaux, Mathematical Modelling of Transformation Plasticity in Steels 1: Case of Ideal-Plastic Phases, International Journal of Plasticity, vol.5, 1989, pp. 551-572.

[15] Chin-Hyung Lee, Kyong-Ho Chang, Finite element simulation of the residual stresses in high strength carbon steel butt weld incorporating solid-state phase transformation, Computational Materials Science, vol.46, 2009, 1014 – 1022.

[16] Ching-Hyung Lee, Computational modeling of the residual stress evolution due to solid-state phase transformation during welding, Modeling and Simulation in Materials Science and Engineering, vol.16, 2008, pp.1 – 16.

[17] K.W. Andrews, Empirical formulae for the calculation of some transformation temperature, J. Iron Steel Res. Int. vol. 203, 1960, pp. 721 – 727.